Impressed Current Cathodic Protection: A useful source for EM exploration?

Tobias Lindau[1] and Michael Becken[1]

[1] *Institut für Geophysik, Westfälische Wilhelms-Universität Münster*

1 Introduction

Many of the pipelines forming the dense system of water-, oil- and gas pipelines present in central Europe are protected against electrochemical corrosion by impressed current cathodic protection (ICCP) systems (Baeckmann et al. (1997), Ahmad (1999)). In normal operation mode an ICCP system injects a DC current into the pipeline in order to achieve protection. However, for occasional pipeline integrity tests the current is switched on- and off periodically, generating time-varying electrical currents and thereby inducing secondary electric- and magnetic fields in the surrounding earth (Bette & Vesper (2005), Grayver et al. (2014)). While to date these fields are considered to be unwanted cultural noise in electromagnetic exploration, this work aims at utilizing the fields generated by the switching of the ICCP current for determining the electrical resistivity of the subsurface. For this purpose we aim at performing electromagnetic field measurements as well as recordings of the injected pipeline current at the injection point. The measured data will be used to calculate transfer functions $\vec{T} = (T_x, T_y)$ describing the relationship between the measured electric fields $\vec{E} = (E_x, E_y)$ and the injected pipe current I:

$$\vec{E}(\vec{r}, \omega) = \vec{T}(\vec{r}, \omega) \cdot I(\omega) \tag{1}$$

For our study we investigate a pipeline segment in northern Germany and begin by determining the current distribution inside such an ICCP protected pipeline. We use the current distribution to create first models of the pipeline source and show first modelling results of the expected electric field distribution in vicinity to the pipeline. Subsequently we use our model to investigate the effect of conudctivity changes in the subsurface on the electric fields recorded at the surface.

2 Working Principle of ICCP Systems

As steel bodies exposed to environmental effects tend to be destroyed by corrosion, pipeline operators make great effort to prevent the destruction of their structures by such processes. While an insulating coating of a steel pipeline greatly reduces the damage caused by corrosion, protection is only achieved as long as the coating is intact. However, due to various factors, defects in the coating do occur along the pipe structure, causing the protection to fail at these locations. Therefore further protection against corrosion is necessary to add protection to the exposed areas of the pipeline as well (e.g. Kutz (2005)).

For this purpose *Cathodic Protection* systems are employed. Such systems are widely used not only for pipeline protection, but are also found in applications linked to the protection of ships hulls or water heaters (e.g. Kutz (2005)). The general idea of *Cathodic Protection* systems is to make the protected structure the cathode of an electrochemical cell. This is achieved by the addition of a suitable material that will act as the anode of the cell and which will be gradually destroyed in favor of the protection of the cathode (e.g. Baeckmann et al. (1997)). A schematic of a simple electrochemical cell, illustrating the principle, is given in Figure 1.

However, while this approach is well suited for smaller structures, it becomes less practical

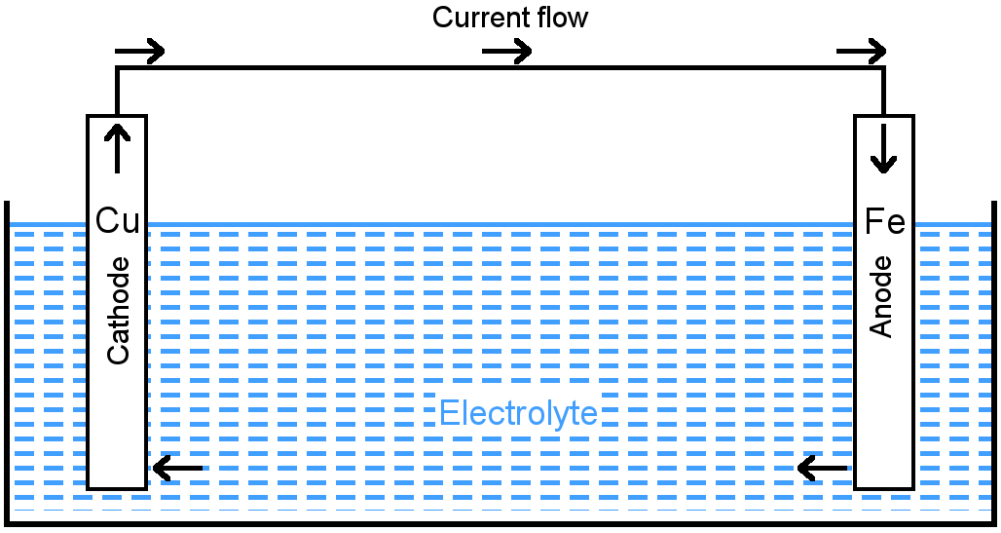

Figure 1: A simple electrochemical cell. Two metals of different electrochemical potential are placed in an electrolyte. Corrosion occurs at the anode, which has a higher energy level (i.e. lower electrochemical potential), whereas no corrosion occurs at the cathode with the lower energy level. Current is flowing through the electrical connection from the cathode to the anode and through the electrolyte from the anode to the cathode. In this example the cell consists of a copper cathode and an iron anode.

when the size of the protected structure becomes larger. Due to the increased amount of current that needs to be supplied by the galvanic anode, larger and more numerous anodes are required, rendering their usage uneconomical. Therefore another approach is pursued, in which a DC power source is added to the system. The power source supplies the additional current needed to protect the structure and which would otherwise have to be supplied by the galvanic anode alone, greatly reducing the anode requirements. Hence the name *Impressed Current Cathodic Protection* (e.g. Kutz (2005)). A schematic of such an ICCP system is shown in Figure 2. While in normal operation mode the current source injects a constant DC current, occasional pipeline integrity tests demand the current to be switched on- and off periodically (e.g. Bette & Vesper (2005)). This switching of the pipe current is automated and sychronized with DCF77 time. Usually a repeating switching pattern of 12 s on- and 3 s offtime is used. The switching of the current generates electromagnetic fields that vary with time and induce secondary electromagnetic fields in the surrounding subsurface. While this switching should be limited to the duration of such integrity surveys, experience has shown that the switching occurs more often. These fields can be measured and are usually considered to be electromagnetic noise. We, however, aim at utilizing these fields generated by the pipeline as sources for exploration purposes.

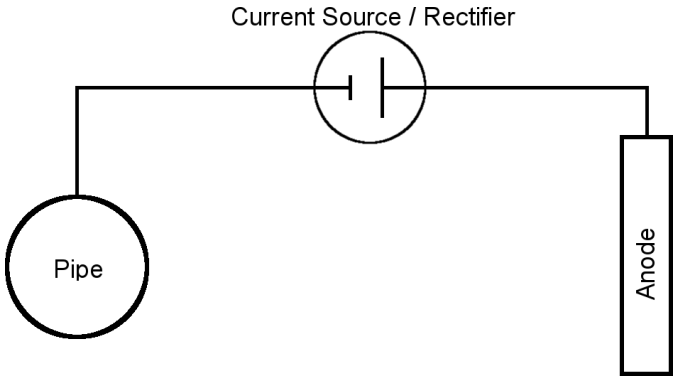

Figure 2: Principle of an ICCP system for pipelines. A DC current source is added to the elctrical connection of pipeline and anode to supply the necessary protection current.

3 Current Distribution

In order to be able to describe and understand the pipeline in terms of an EM source it is necessary to understand the current flow within the pipeline. While for the standard sources used in CSEM a uniform current flow is assumed, this assumption cannot be applied to pipeline sources. As coating defects occur along the pipeline, current flowing through the pipe and towards the anode will leak into the surrounding soil at various locations along the pipeline path. This leaking causes the current flow to decay towards the end, resulting in a non-uniform current flow within the pipeline. As the information about the current flow is not of primary interest for the pipeline operator but only the pipe potential relative to its surrounding (e.g. Bette & Vesper (2005)), there is no data avaiable and field measurements need to be performed in order to determine the current distribution.

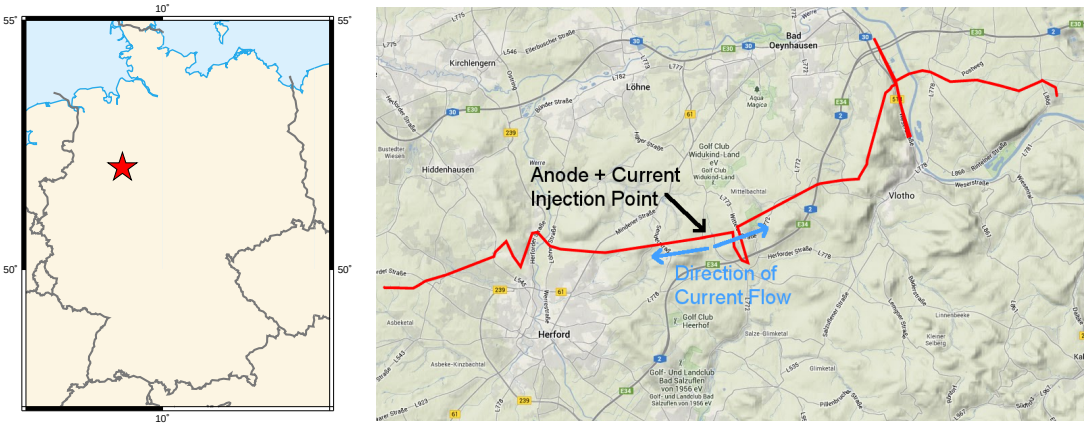

Figure 3: **Left:** Map of Germany with the location of the test segment marked by a star. **Right:** Map view of the area in which the pipeline is located with the approximate pipeline path and the locations of the current injection point and the anode drawn in. Source: maps.google.com

For our studies we chose a pipeline segment near Herford, Germany which is operated by the Westnetz GmbH (see Figure 3). It is approximately 30 km long and consists of a bitumen coated steel pipe with a diameter of 0.3 to 0.4 m. It is protected by a rectified

50 Hz current of 2.5 A. The anode and the current injection point are located in the approximate center of the pipeline segment, causing the current to split up in order to protect both branches of the pipe.
The current flow within the pipeline cannot be measured directly as it is buried and thereby cannot be accessed. To measure the current in the buried pipeline from the surface two measurement methods were applied. In a first approach the total magnetic fields along profiles crossing the pipeline perpendicularly were measured for active and inactive ICCP current. The difference in the total magnetic field was considered to be caused by the DC current flow withing the pipe as described by the law of Biot-Savart (e.g. Stratton (1941)). We then attempted to invert the gathered magnetic field data for the current strength, depth and additional parameters at the individual profile location. However, the data could be explained equally well by a number of parameter sets, making it impossible to make definite and unbiased statements about the current distribution. Subsequently the data was discarded.
The second measurement method also utilizes the magnetic fields generated by the current flow, but uses time variational magnetic field rather than the static magnetic field. Since the ICCP current consists of a rectified 50 Hz current, the DC current flowing in the pipe has a frequency of 100 Hz. The resulting magnetic field at this frequency is measured using two induction coils located in different heights above the pipeline, allowing to calculate the pipe depth as well as the current strength. The measurements were performed using a *RD400* pipeline detection tool supplied by Westnetz. The measurements took place at 47 locations located along the pipeline path. The results for the current from the measurement are shown in Figure 6.
The data shows the expected decay of current towards both ends of the pipeline. However, the maximum current amplitudes of both branches, directly at the injection point, do not add up to the expected injected current of 2.5 A. In order to evaluate the data measured by the *RD400* and check for possible corrections that may be needed to be applied to the data, calibration measurements were performed. For this purpose a cable was fed with a recitfied 50 Hz current similar to the pipes ICCP current.

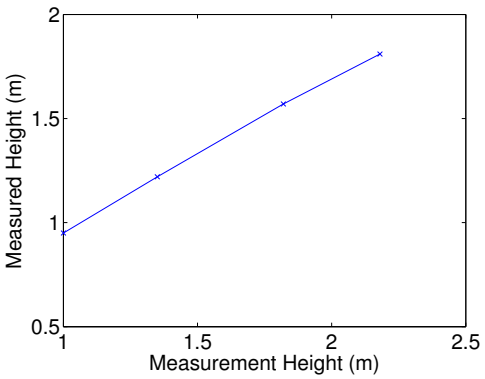

Figure 4: Results of the calibration measurements. Shown is the real- and the measured height for an injected current of 1 A

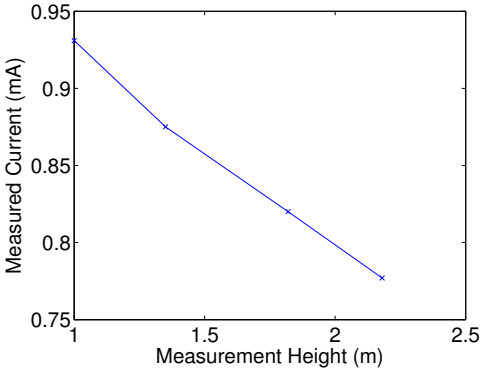

Figure 5: Results of the calibration measurements. Shown is the current that was measured at differents heights for an injected current of 1 A

The *RD400* was used to measure the current within the cable as well as the height above the cable for various combinations of measurement heights and current strengths. The data shows a strong dependence of the measured currents and heights from the distance to the cable (Figure 4 and 5). As the measured heights do not show dependence on the

injected current, a simple relationship between the measured height and real measurement height was derived and used to correct the measured currents depending on the measured height.
Assuming this relationship is valid for the pipeline data as well, the pipeline data was corrected using the same relationship. The resulting current distribution along the pipeline is depicted in Figure 6 along with the originally measured data. The peak values of both branches now add up to a value closer to the expected values of 2.5 A, indicating that the corrections give reasonable results. In general the current shows exponential decay away from the injection site and an exponential function is fitted to the data in order to be able to make statements about the current at locations where no measurements took place.

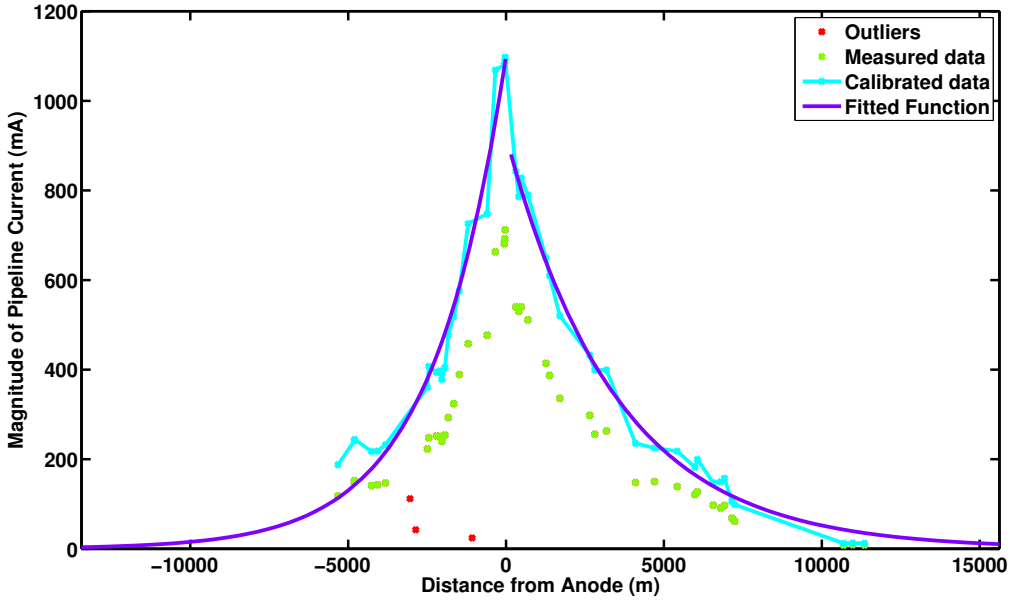

Figure 6: Data from the measurement of the pipe current using the RD400 pipeline detection tool. Shown is the originally measured data (red + green). The red datapoints are discarded as outliers. The data corrected by the function derived from the calibration measurements is shown in green. The purple line represents the function fitted to these points, describing the current distribution as it is used for our models.

4 Modelling Results

To get an impression of the electric fields generated by the pipeline, forward calculations were performed using the current distribution obtained from the calibrated data. The calculations were performed in 1D using the software EM1D which is capable of modelling the fields of various electric- and magnetic type sources for a layered resistivity distribution (Streich & Becken, 2011b). In our model the pipeline is represented by 101 finite wire sources to approximate the pipeline geometry and to incorporate the non-uniform current distribution (Streich & Becken, 2011a). The length of the individual wire sources does not exceed a length of 500 m. Each source is assigned a constant current value which is determined from the exponential function fitted to calibrated current data by calculating the mean current for the section of pipeline represented by the respective element.
Two resistivity distributions were considered: The first resistivity model consists of a

homogeneous half space of 7 Ωm resistivity, whereas the second model adds a 100 m thick conductive layer of 1 Ωm in 500 m depth to the homogeneous model. For the first model the resulting electric field components E_x and E_y at the surface are shown in Figure 7 for a evaluation frequency of 1 Hz.

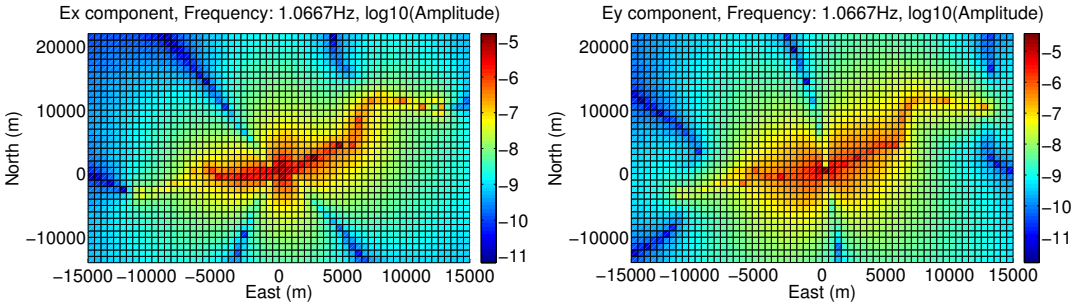

Figure 7: Shown are the electric field amplitudes at the surface resulting from the forward modeling at a frequency of 1 Hz for a homogeneous half space of 7 Ωm.
Left: Amplitude of E_x-component. **Right:** Amplitude of E_y-component.

The electric fields excited by the source are clearly visible and well within the measurable range. In addition, a comparison of the E_y amplitudes of both models, as shown in Figure 8, reveals a strong influence of the conductive layer on the electric fields amplitudes. This indicates sensitivity of the fields to conductivity changes in the subsurface in this depth.

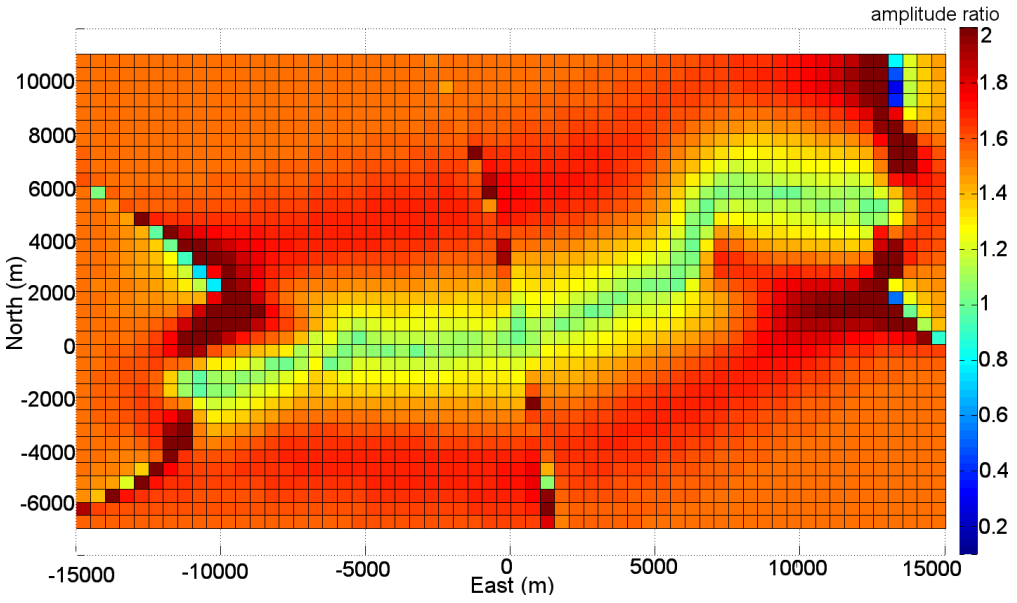

Figure 8: Comparison of the amplitude of E_y components from both models. Shown is the amplitude ratio given by $|E_{y,hom}|/|E_{y,cond}|$, where the subscript *hom* denotes the fields of homogeneous resistivity model and *cond* the values of the model with the conductive layer.

5 Conclusion

The current distribution within the pipeline can easily be determined by measurements with a pipeline detection tool similar to the RD400 device used in this study. The exponential current decay determined for the investigated pipeline segment confirms the expectation that the assumption of a uniform source current distribution is not applicable to pipeline sources.
Modelling of the pipeline source by using a number of finite wire sources and assuming a cascading source current yields resonable models for the electric fields generated by such a source. The electric field amplitudes of the model suggest that field measurements will be able to pick up the signals originating from such a source.
Field measurement, during which the electromagnetic fields and the injected current were recorded, have already been performed and are currently being analyzed. Signals originating in the switching of the pipelines ICCP current are clearly visible in the electric field data. Preliminary processing results give promising results and seem to be in good agreement with the models presented here. We plan, however, to perform additional field measurements along additional profiles to further map the electromagnetic field distribution.

References

Ahmad, Z. (1999). *Principles of corrosion engineering and corrosion control.* John Wiley & Sons Canada, Limited.

Baeckmann, W. von, Schwenk, W., & Prinz, W. (1997). *Handbook of cathodic corrosion protection.* Elsevier Science.

Bette, U., & Vesper, W. (2005). *Taschenbuch für den kathodischen korrosionsschutz.* Vulkan-Verlag.

Grayver, A., Streich, R., & Ritter, O. (2014). 3d inversion and resolution analysis of land-based csem data from the ketzin storage formation. *GEOPHYSICS*, *79*(2), E101-E114.

Kutz, M. (2005). *Handbook of environmental degradation of materials.* Elsevier Science.

Stratton, J. (1941). *Electromagnetic theory.* McGraw-Hill book Company, Incorporated.

Streich, R., & Becken, M. (2011a). Electromagnetic fields generated by finite-length wire sources: Comparison with point dipole solutions. *Geophysical Prospecting*, *59*(2), 361-374.

Streich, R., & Becken, M. (2011b). Sensitivity of controlled-source electromagnetic fields in planarly layered media. *Geophysical Journal International*, *187*(2), 705–728.